Effluent Concentration Profiles in Centrifugal Partition Chromatography

M. J. van Buel, L. A. M. van der Wielen, and K. Ch. A. M. Luyben
Dept. of Biochemical Engineering, Delft University of Technology, 2628 BC Delft, The Netherlands

Centrifugal partition chromatography (CPC) is a relatively new preparative chromatographic technique. To understand, predict, and optimize CPC separations a model is needed, describing the effluent concentration profile as a function of the phenomena that determine the separation efficiency (mass transfer, mixing, and partitioning). The model presented in this article describes experimental effluent concentration profiles accurately. Partition coefficients, Stanton numbers, and Péclet numbers were obtained by comparing model simulations to experimental pulse-response data. The fitted partition coefficients agree well with those obtained from shake-flask experiments. Mass-transfer limitation is the major reason for peak broadening. The inverse mass-transfer coefficient is a linear function of the partition coefficient. The model will be a valuable tool in determining the influence of mass transfer as a function of various experimental conditions.

Introduction

Centrifugal partition chromatography (CPC) is a novel chromatographic technique in which the separation mechanism is based on the difference in partitioning of solutes over two immiscible liquid phases (Berthod and Armstrong, 1988a). Figure 1 shows a CPC. It consists of cartridges of stacked polymer plates, which are placed in a centrifuge and in which channels connected by narrow ducts are engraved. The stationary phase, differing in density from the mobile phase, is retained in the channels due to the combination of the centrifugal force and the tortuous column geometry. Via the ducts, where no stationary phase is present, the mobile phase flows from one channel to the next. Due to the centrifugal force the stationary phase will not leave the channel together with the mobile phase, while it is also impossible for the stationary phase to leave the channel at the opposite side, due to the inflow of the mobile phase. When the mobile phase is the denser phase, it will flow away from the axis. This is called the "descending" mode. When the mobile phase is the lighter phase, it will flow in the direction of the axis. This is called the "ascending" mode. The mobile phase is pumped through the stationary phase in the form of droplets, jets, or breaking jets, depending on operating conditions, as demonstrated by van Buel et al. (1995).

Components introduced as a mixture in the mobile phase, partition differently over the two phases, and consequently leave the column separated. A column can consist of 800 or more channel–duct combinations. The total volume of a commercial CPC column ranges from 40 mL for a semianalytical column to over 30 L for a preparative column (Sanki). Different cartridge and channel geometries are available (Foucault, 1995). Any mixture of liquids, forming a two-phase system with a density difference between the phases, can be applied in principle. This enables fine-tuning of the separa-

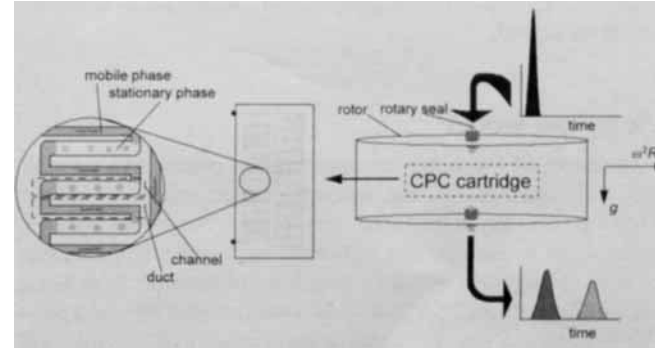

Figure 1. Centrifugal partition chromatograph.

Correspondence concerning this article should be addressed to L. A. M. van der Wielen.

tion system to a specific mixture of components to be separated. The carrying capacity of the liquid phases is limited only by the solubility of the solutes in either phase. This makes CPC a promising alternative for conventional preparative chromatography, which is limited by the saturation capacity of the stationary sorbent material. Numerous examples of separations, performed by CPC, are given by Foucault (1991) and Marston and Hostettmann (1994). An extensive list of literature on CPC separations and equipment is given by Conway (1995).

Until now optimization of a CPC separation is mainly performed by qualitative means. Although retention times can be predicted from measured partition coefficients (Gluck and Martin, 1990), the prediction of peak broadening is still difficult. Quantitative information about the phenomena involved in the retention and peak broadening must be available, to predict and optimize the efficiency of a CPC separation.

Armstrong et al. (1988) have shown that the efficiency relationships that are available for conventional chromatographic separations do not directly apply for CPC, due to the fact that several phenomena that are important for band broadening in conventional chromatography do not apply for CPC. Furthermore, they indicate that mass-transfer resistance in the mobile and the stationary phase most likely is responsible for the observed decrease in efficiency as a function of the flow rate. Based on this insight, they derived a relation for the separation efficiency (defined as the ratio of the change in concentration of solute actually occurring in the mobile phase over the change that would occur in the mobile phase if the system were allowed to reach equilibrium) based on mass transfer of a component between two phases. However, their model did not predict effluent concentration profiles (complete chromatograms) and does not account for peak broadening due to mixing inside (dispersion) and outside the column (off-column mixing). Still, the engineering approach of these authors greatly improved the understanding of CPC separations.

van Buel et al. (1996) presented a model assuming that the retention of a peak is caused by partitioning over two phases, while peak broadening is only caused by mass-transfer limitation. The analytical solution of the model can be used to predict the effluent concentration profiles, when a partition coefficient and an overall mass-transfer coefficient are known. However, the model does not account for peak broadening due to dispersion and off-column mixing. In this article, an extension of our previous model (van Buel et al., 1996) (now including off-column mixing and dispersion), and a thorough experimental verification are presented. Furthermore, the relative importance of the phenomena causing band broadening is examined.

Plug-Flow Model

In modeling the effluent concentration profile of a component (chromatogram), the following assumptions are made. First, it is assumed that the only reason for retention of a component is partitioning between the mobile and the stationary phases, and no other sorption mechanisms have been taken into account. Second, it is assumed that the composition (concentration and type of component) of the injected sample does not influence the partition coefficient of the individual components or the equilibrium composition of the two-phase system. This assumption is usually valid for low component concentrations, but may not hold for higher concentrations.

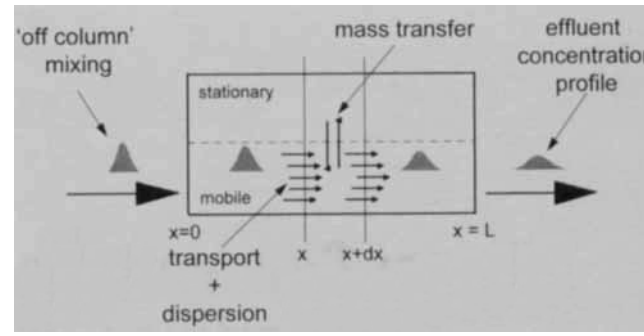

Figure 2. CPC model.

Third, mixing in the stationary phase as a whole is neglected. The fact that the column consists of 800 or more individual and separate channels supports this assumption, even if the stationary phase in the individual channels is ideally mixed, this will hardly affect peak broadening. The mobile-phase mixing is described by an axial dispersion contribution. Due to the tortuous shape of the column, it is practically impossible to predict the dispersion in the mobile phase. Therefore, dispersion is characterized experimentally, as a function of the experimental conditions, by injecting a component that does not partition to the stationary phase (unretained component). Peak broadening of this component is therefore caused by dispersion in the mobile phase only. Finally, it is assumed that mass transfer can be described by a linear driving-force model (Lewis and Whitman, 1924).

Based on these assumptions, the mobile phase is described as plug flow with axial dispersion, and the stationary phase as nonmixed (Figure 2). The resulting set of partial differential equations describing the concentration of a solute in the bulk of the mobile and the stationary phase (C_m and C_s) as a function of the axial position in the column, x, and the time, t, reads as follows:

$$\frac{\partial C_m}{\partial t} - D_{ax}\frac{\partial^2 C_m}{\partial x^2} + \upsilon\frac{\partial C_m}{\partial x} = -\frac{k_m a}{1-\epsilon_s}(C_m - C_m^*) \quad (1)$$

$$\frac{\partial C_s}{\partial t} = \frac{k_s a}{\epsilon_s}(C_s^* - C_s) \quad (2)$$

in which D_{ax} is the axial dispersion coefficient, υ is the velocity of the mobile phase, ϵ_s is the volume fraction of stationary phase in the column (the stationary phase holdup), a is the specific interfacial area between the mobile and the stationary phases, k_m and k_s are the local mass-transfer coefficients in the mobile and the stationary phases, and C_m^* and C_s^* are the interfacial concentrations at the mobile and the stationary phase sides of the interface. The boundary conditions are

$$C_s(t=0,x) = 0 \quad (3)$$

$$C_m(t=0,x) = 0 \quad (4)$$

$$C_m(t, x=0) = \delta \tag{5}$$

$$\lim_{t \to \infty} C_m = 0, \tag{6}$$

where δ indicates a Dirac pulse. Eliminating the unknown interface concentrations by using the bifilm model of Lewis and Whitman (1924) leads to

$$\frac{\partial C_m}{\partial t} - D_{ax}\frac{\partial^2 C_m}{\partial x^2} + v\frac{\partial C_m}{\partial x} = -\frac{k_o a}{1-\epsilon_s}(KC_m - C_s) \tag{7}$$

$$\frac{\partial C_s}{\partial t} = \frac{k_o a}{\epsilon_s}(KC_m - C_s). \tag{8}$$

The partition coefficient (K) is defined as

$$K = \frac{C_s^{eq}}{C_m^{eq}}, \tag{9}$$

where C_s^{eq} and C_m^{eq} are the concentration of the stationary and the mobile phase when the two phases are in equilibrium.

The overall mass-transfer coefficient (k_o) is defined as

$$\frac{1}{k_o} = \frac{K}{k_m} + \frac{1}{k_s}. \tag{10}$$

The product of the overall mass-transfer coefficient and the specific interfacial area is called the overall volumetric mass-transfer coefficient ($k_o a$). Introducing the following dimensionless variables:

$$X = \frac{C_m}{C_m^o} \tag{11}$$

$$Y = \frac{C_s}{KC_m^o} \tag{12}$$

$$z = \frac{x}{L} \tag{13}$$

$$\Theta = \frac{t}{\tau}, \tag{14}$$

in which C_m^o is the concentration of the component in the injected sample; X and Y are dimensionless concentration in mobile and stationary phases, respectively; z is the dimensionless position in the column; Θ is the dimensionless time; L is the column length; and τ is the residence time of the mobile phase, leads to the following set of dimensionless partial differential equations:

$$\frac{\partial X}{\partial \Theta} - \frac{1}{Pe}\frac{\partial^2 X}{\partial z^2} + \frac{\partial X}{\partial z} = -St\,K(X-Y) \tag{15}$$

$$\frac{\partial Y}{\partial \Theta} = \frac{(1-\epsilon_s)}{\epsilon_s} St\,(X-Y). \tag{16}$$

The Stanton number (St) and the Péclet number (Pe) are defined as

$$St = \frac{k_o a V}{\phi_v} \tag{17}$$

and

$$Pe = \frac{vL}{D_{ax}} \tag{18}$$

where ϕ_v is the mobile phase flow rate, and V is the column volume. The model contains four parameters: St, Pe, ϵ_s and K, of which only Pe and St have to be determined by fitting experimental effluent concentration profiles. The overall volumetric mass-transfer coefficient can be calculated from St if the column volume and the flow rate are known.

Off-column mixing and numerical solution

Part of the broadening of an effluent concentration profile is due to mixing outside the column (off-column mixing). If the additional peak broadening is not corrected, it will lead to Péclet and Stanton numbers that are incorrect. Therefore, the set of partial differential equations (Eqs. 15 and 16) has to be solved for an arbitrary input concentration profile. This is done by solving the set of differential equations for X (dimensionless mobile-phase concentration) in the Laplace domain and transforming the solution to the Fourier domain. In the Fourier domain, the transformation function, $\tilde{X}$, is multiplied by a Fourier transformed experimental input concentration profile, $\tilde{I}$, obtained without the column present in the experimental setup, giving a predicted effluent concentration profile in the Fourier domain, $\tilde{O}$. By doing so, peak broadening due to off-column mixing is included in the model. Then the effluent concentration profile is transformed back to the time domain, O. By comparing the experimental concentration profile obtained with the column, E, to the simulated concentration profile in the time domain, O, it is possible to obtain values for the partition coefficient, the overall volumetric mass-transfer coefficient, and the Péclet number if the stationary phase holdup, the flow rate, and the total volume are known.

The input concentration profile that is measured without the column present in the experimental setup, measures both peak broadening before the column, $I_{\text{before column}}$ (due to pressure transmitter, injector, upper rotary seal, and tubing), as well as peak broadening behind the column, $I_{\text{behind column}}$ (due to lower rotary seal, water bath, UV meter, and tubing). Because of the convolution principle it is possible to treat the two peak-broadening phenomena as one in the Fourier domain since:

$$\tilde{I}_{\text{before column}} \times \tilde{X} \times \tilde{I}_{\text{behind column}} = \tilde{I}_{\text{before column}} \times \tilde{I}_{\text{behind column}} \times \tilde{X} = \tilde{I} \times \tilde{X}. \tag{19}$$

This procedure is shown graphically in Figure 3. Additional literature on this specific method of solving sets of linear partial differential equations can be found, among others, in Hsu and Chen (1987) and Brigham (1988). The solution in the Fourier domain is derived in the Appendix.

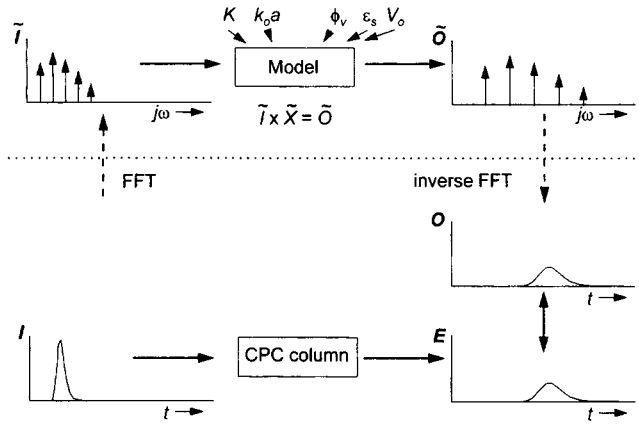

Figure 3. Fourier fit method.

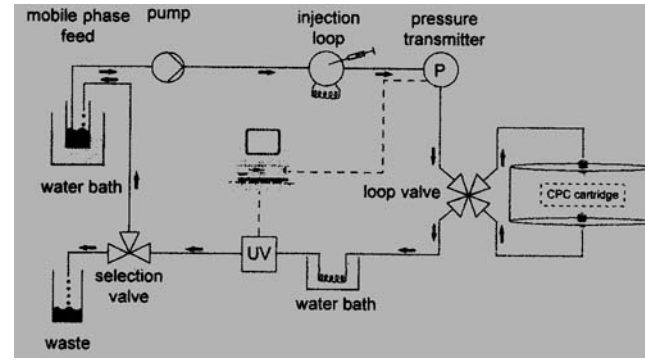

Figure 4. Experimental setup.

Materials and Methods

Apparatus

Chromatographic experiments were performed with a CPC-LLN cartridges type 250 W, purchased from Sanki Engineering Ltd., placed in a rotor constructed by the workshop of our department. The column consists of 2 to 6 cartridges with 400 channels each. Each cartridge has a volume of 20.2 $\pm$0.2 mL. The distance between the axis and the center of the cartridge was 0.21 m. A more detailed description of the 250 W cartridge is given by Foucault (1995) and van Buel et al. (1995).

Materials

Methanol (> 99.8%) was purchased from Acros, Geel, Belgium and *n*-heptane (> 99%) was purchased from Merck, Darmstadt, Germany. Water was demineralized. Three different two-phase systems were used for the experiments: heptane/methanol/water–50/37.5/12.5 vol % (HMW 12.5), heptane/methanol/water–50/25/25 vol % (HMW 25), and heptane/methanol/water–50/12.5/37.5 vol % (HMW 37.5). The solutes that were used as model components are given in Table 1.

Operating the CPC column

A drawing of the experimental setup appears in Figure 4. An experiment was started by rinsing the tubing, the column, and the pressure-drop meter with acetone and filling the column with stationary phase. During all the experiments the top phase (heptane rich) was used as the stationary phase in the descending mode. Subsequently, the column was bypassed by closing the loop valve, and the equipment was rinsed with acetone and filled with mobile phase. Then the centrifuge was started at the lowest rotational frequency to be used during the experiments, the loop valve was opened, and the mobile phase was pumped through the column at the highest flow rate to be used during the experiments. This procedure of filling the column reduces leaking of stationary phase from the column during the experiments. The stationary-phase holdup of the column was measured by collecting the stationary phase that flows from the column during filling with the mobile phase. Since the volumes of the individual parts of the setup are known, it is possible to calculate the stationary-phase holdup, corrected for the volumes before and after the column. The pump was a Shimadzu LC8A. The temperature of the mobile phase was kept at 25°C in a water bath.

The stationary-phase holdup of the column was monitored during the experiments with a pressure-drop meter (Bourdon Sedeme E713). The solutes were injected (diluted with mobile phase) with a Rheodyne 7125 high-pressure injecting valve with a sample loop of 220 μL, and detected by UV spectrophotometry with a Biorad Econo UV monitor at 254 or 280 nm. The temperature of the mobile phase was increased to 45°C just before the UV meter to increase base-line stability. The concentrations of the injected samples were in the range of 4–22 g/L.

Preparing the two-phase system

The phase systems were prepared by shaking appropriate amounts of the separate liquids, shaking them vigorously, and letting them equilibrate overnight in a water bath at 25°C.

Table 1. Supplier and Purity of Model Components

Component	Supplier	Purity
1,3,5-Trihydroxybenzene	Fluka AG	Unknown
Phenol	Fluka Biochemika	> 99.5
4-Chloro-3-methylphenol	Aldrich-Chemical Co.	Unknown
2-Phenyl-1-ethanol	Fluka-Chemika	> 99%
2-Ethylphenol	Janssen Chemica	99%
2,4-Dimethylphenol	Fluka AG	≈ 90%, 5.7% 2,5-dimethylphenol
2,6-Dichlorophenol	Aldrich-Chemie	> 99%
2,4-Dichloro-5-methylphenol	Aldrich Chemical Co.	Unknown
Benzaldehyde	Merck, Schuchardt	> 99%

The two-phase system was poured into a separation funnel and the two phases were separated. The mobile phase was deareated by pouring it over a G4 glass filter while applying a vacuum.

Partition coefficients by shake-flask experiments

Shake-flask experiments were performed to determine the partition coefficient of a component by weighing a small amount into the equilibrated two-phase system (±10 mL of each phase in Chrompack bottles of 50 mL with a Teflon cap) and stirring vigorously (with a magnetic stirrer) overnight in a water bath at 25°C. After removal from the water bath the phases were separated immediately and analyzed by gas chromatography. The experiments were performed in duplicate. The initial concentration of the components was 0.4 g/L mobile phase.

Results and Discussion

The input concentration profile

To compensate for peak broadening due to mixing in the rotary seals, tubing, pressure transmitter, and injection loop (off-column mixing), a concentration profile measured with the column removed from the setup was used as the input concentration profile (I) for the model. Experimentally, it was shown that the normalized input concentration profile ($E = 1$) is independent of the injection volume, the type of solute, or the concentration of the solute (within the range of experimental conditions). The input concentration profile with the column removed from the setup is, of course, a function of the flow rate. However, all normalized effluent concentration profiles were identical (within the experimental error) as a function of $t\phi_v$. This means that only one form of input concentration profile is needed for a given experimental setup.

Comparing model predictions to experimental CPC chromatograms

A typical chromatogram is shown in Figure 5. Pulse-response experiments for various experimental conditions and components were performed. The model predictions were compared to the experimental effluent concentration profiles to determine the partition coefficient, the Stanton number, and the Péclet number. Before the calculations, the experimental effluent concentration profiles were normalized ($E = 1$).

The effluent concentration profiles (with the column present in the setup) of components that partition to the stationary phase ($K \neq 0$) were shown, experimentally, to be independent of the feed concentration in the range 4–22 g/L for the components given in Table 1. At higher concentrations, the effluent concentration profiles start to show increased tailing. The reason for this phenomenon is not clear, but might be caused by overloading (exceeding the maximum solubility) of the stationary phase.

Berthod and Armstrong (1988b) indicated that larger injection volumes (2–10 mL) may affect the peak shape. However, in the range that was used for the experiments in this work (0–220 μL injection volume) no effect on the effluent concentration profile was observed.

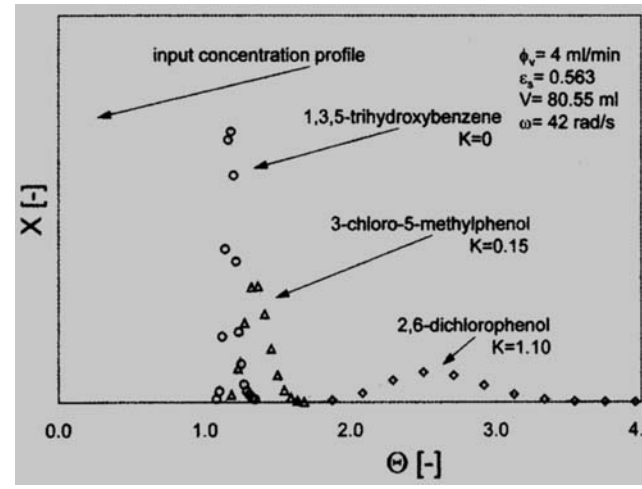

Figure 5. Fit of the model to experimental effluent concentration profiles of THB, CMP and DCP for the HMW 25 two-phase system.

Curves are experimental data, markers are model predictions.

Determining both the Stanton and the Péclet numbers by fitting the model to an effluent concentration profile of a single component leads to undesirably large errors; in particular for the Péclet number. Therefore, the Péclet number was determined by fitting the model to the effluent concentration profile of an unretained component (1,3,5-trihydroxybenzene (THB), $K < 0.0015$). Since THB hardly partitions to the stationary phase, peak broadening is only due to off-column mixing and dispersion in the mobile phase. Fitting the Péclet number was done with the model without partitioning ($K = 0$). The THB effluent concentration profiles can be fitted with 1 parameter (Pe). However, to compensate for a possible (small) error in the measured stationary phase holdup, both the Péclet number and the stationary-phase holdup were fitted.

The partition coefficient and the overall volumetric mass-transfer coefficient of a component with $K \neq 0$ were fitted with the model, including dispersion, mass transfer, and partitioning. The Péclet number and the stationary-phase holdup were set at a fixed value, determined by fitting the effluent concentration profile of an unretained component (THB) measured at the same experimental conditions, as described earlier.

Figure 5 shows the result of a model fit to an experimental concentration profile for THB, 4-chloro-3-methylphenol (CMP) and 2,6-dichlorophenol (DCP) in HMW 25 at 4 mL/min, 42 rad/s, and a stationary-phase holdup of 0.56. The difference between the model predictions and the experimental effluent concentration profiles was generally minimal.

Influence of mobile-phase mixing on the effluent concentration profile

To study the influence of mobile-phase mixing, Péclet numbers were determined for various experimental conditions. The Péclet number for a given experimental condition was obtained by fitting the model to the experimental effluent concentration profile of THB. For all THB pulse-

Table 2. Péclet Number for Various Experimental Conditions for the HMW 25 System

ϕ_v mL/min	ϵ_s	ω rad/s	V mL	Pe (s.d.)
4	0.56	42	40.4	4,600 (2,100)
4	0.56	58	40.4	3,700 (340)
4	0.56	87	40.4	6,200 (780)
4	0.56	106	40.4	5,600 (730)
4	0.56	42	80.6	4,200 (400)
4	0.56	42	121.2	8,000 (500)
1	0.56	42	40.4	7,200 (1,110)
2	0.56	42	40.4	3,300 (400)
3	0.56	42	40.4	4,300 (390)
4	0.27	42	40.4	2,300 (30)
4	0.39	42	40.4	2,500 (110)
4	0.47	42	40.4	2,700 (440)

response experiments, the stationary-phase holdup obtained from the fit-procedure was within 0.3% of the stationary-phase holdup measured with the burette method, indicating that both the burette method and injecting a component with a very low partition coefficient give a very similar value for the stationary-phase holdup. Another method to determine the stationary-phase holdup is given by Gluck and Martin (1990).

Table 2 gives fitted Péclet numbers for various flow rates, rotational accelerations, column volumes, and stationary-phase holdups for the HMW 25 system. The fitted Péclet numbers are obtained by averaging the results from fitting 3 to 4 different THB peaks by using 2 to 3 different input-concentration profiles. The fitted Péclet numbers are very large (> 2,000). The large standard deviations in the Péclet numbers might be caused by the fact that the additional peak width due to dispersion, compared to the peak width due to off-column mixing, is only 10–30% (depending on the experimental conditions). Due to the large experimental error it is not possible to show a trend in the Péclet number as a function of the various operating conditions. The average Péclet number for a given experimental condition will be fixed while fitting the partition coefficient and the overall volumetric mass transfer coefficient.

Partition coefficients determined by CPC vs. partition coefficients determined by shake flask

To determine the influence of the concentration on the partition coefficients of components in the HMW 25 system, partition coefficients for phenol, CMP, DCP, and 2,4-dichloro-5-methylphenol (DCMP) were determined as a function of the concentration by the shake-flask method. The result is shown in Figure 6. The error in the measured partition coefficients is roughly 5% (based on the mass-balance deficiency). The partition coefficients for these components are almost independent of the concentrations used for the HMW 25 system. Since the concentration of the injection samples (4–22 g/L) is within the range used for the shake-flask experiments, it is expected that the partition coefficient of a component will also be constant over the column.

Figure 7 shows that the partition coefficients, determined by fitting the model to the experimental concentration profiles (K_{CPC}), compare well with the partition coefficients determined by the shake-flask method (K_{SF}) for the HMW 12.5,

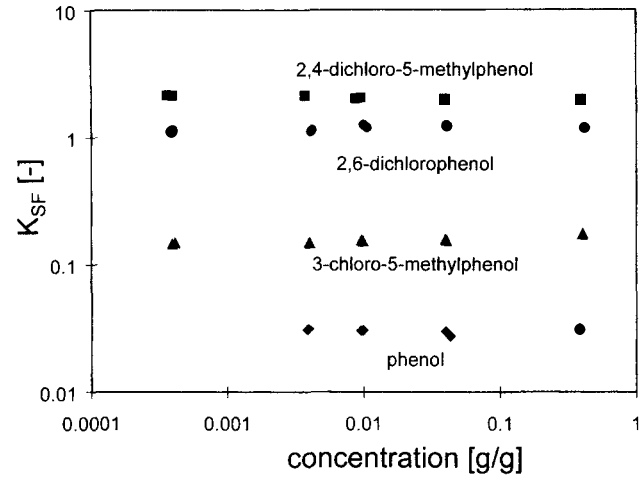

Figure 6. Partition coefficient determined by shake-flask experiments (K_{SF}) as a function of the concentration of a solute in g/g two-phase system.

HMW 25, and the HMW 37.5 systems. The average error in the partition coefficient (K_{CPC}) determined by fitting the CPC experiments is roughly 10%. This was already shown for the heptane/water and the octanol/water system by Berthod and Armstrong (1988a), Gluck and Martin (1990), El Tayar et al. (1991), and Berthod et al. (1992). However, they used the retention time (top of the peak) for calculating the partition coefficient. This is only correct if the peaks are perfectly symmetrical, which is not always the case for CPC. Figure 5 shows that mass-transfer limitation and dispersion causes a tailed concentration profile. This means that the mass average retention time (first moment) of the peak should be used to calculate the partition coefficient. However, the deviation from the symmetrical peak is so small that the results are nearly the same.

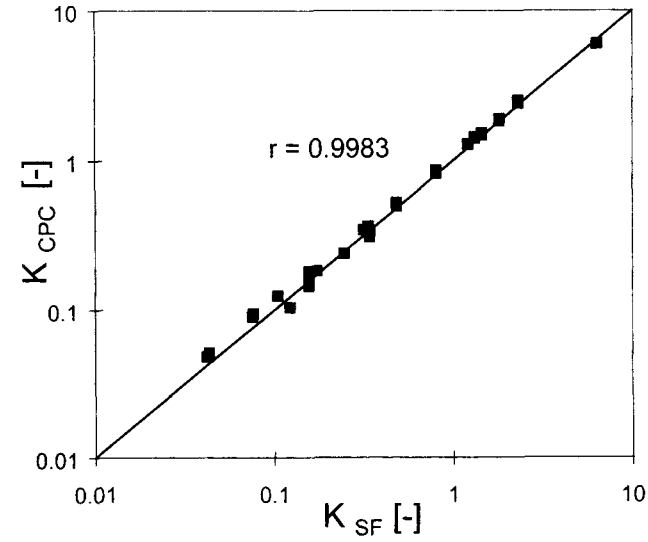

Figure 7. Parity of partition coefficient determined by fitting CPC effluent concentration profiles and partition coefficient from shake-flask experiments.

Overall volumetric mass-transfer coefficient as a function of the partition coefficient

The inverse overall volumetric mass-transfer coefficient is expected to be a linear function of the partition coefficient as indicated by Eq. 10. Since it is not possible (as yet) to determine the specific interfacial area (a) in a fast-spinning CPC column, the overall mass-transfer coefficient (k_o) cannot be calculated independent of a. To check whether or not Eq. 10 is valid for CPC separations, various pulse-response experiments for components with different partition coefficients have been performed with the HMW 25 system at 4 mL/min, 41 rad/s, a column volume of 40.4 mL, and a stationary phase holdup of 0.56. The results are shown in Figure 8. The error in the overall volumetric mass-transfer coefficient was estimated from repeated injections with CMP (the column was flushed and filled between each experiment) to be smaller than 10%. Apart from 2-phenylethanol, the inverse overall volumetric mass-transfer coefficient is a linear function of the partition coefficient as represented by Eq. 10, within the experimental error. The deviation of 2-phenylethanol might be due to its very low partition coefficient. For 2-phenylethanol the additional peak broadening due to mass-transfer limitation (in addition to the peak broadening due to dispersion) is relatively small. This might lead to a larger error in the fitted overall mass-transfer coefficient. Possible deviations from Eq. 10 might also be explained by the fact that although the hydrodynamic conditions are equal for all components, the difference in molecular properties (e.g., mass, size), might lead to slight differences in the diffusion coefficients in both phases for a component, and therefore in the overall volumetric mass-transfer coefficients. The fitted values for $1/k_s a$ and $1/k_m a$ are 12.0 ± 1.2 and 20.0 ± 1.4 s, respectively.

For high overall volumetric mass-transfer coefficients the effluent peak is sharp. For infinitely high overall volumetric mass-transfer coefficients, the peak width will become equal to the peak of an unretained component. Figure 9 shows simulated concentration profiles for three relatively low values of the overall volumetric mass-transfer coefficient (0.01, 0.05, and 0.25 s^{-1}). For these low overall volumetric mass-transfer coefficients the peak is very broad and diluted. Hence, the overall volumetric mass-transfer coefficient has a large effect on peak broadening, and therefore on the efficiency of a separation.

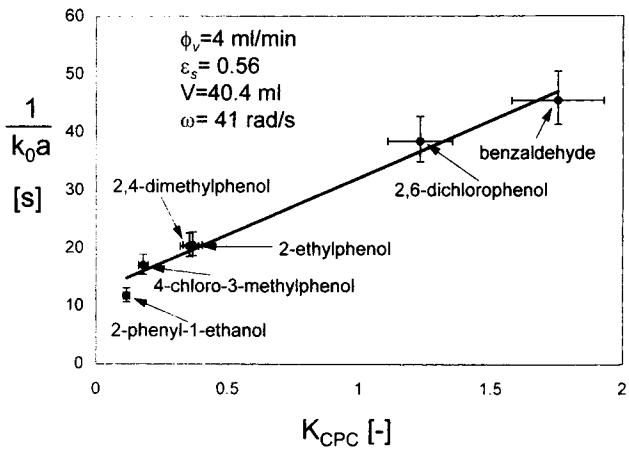

Figure 8. Inverse overall volumetric mass-transfer coefficient as a function of the partition coefficient.

Both are fitted on experimental effluent concentration profiles. Markers are data, the line is according to Eq. 10.

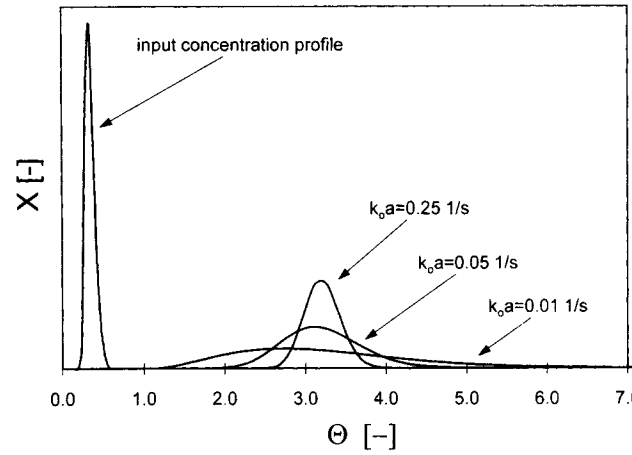

Figure 9. Model simulations for various overall volumetric mass-transfer coefficients.

$\phi_v = 4$ mL/min; $\epsilon_s = 0.65$; $K = 1$; $V = 40.4$ mL; $Pe = 4{,}550$.

Influence of column dimensions on the overall volumetric mass-transfer coefficient

Since CPC is a preparative technique, it is interesting to know how $k_o a$ changes when the volume of the column is increased, by increasing the length of the column (number of cartridges), or by increasing the dimensions (length, height, and width) of the individual channels. When the length (volume) of the column is increased, the specific interfacial area ($a = A/V$) is expected to be constant, since both the interfacial area (A) and the column volume (V) increase to an equal extent. Therefore, $k_o a$ is also expected to be constant, since the column length (number of channels) for the same experimental conditions has no influence on k_o. Table 3 gives the overall volumetric mass-transfer coefficients for CMP and DCP for three different column volumes for the system HMW 25 at 4 mL/min and 41 rad/s. The cartridges were filled each time at 5 mL/min and 30 rad/s to obtain the same stationary-phase holdup of 0.57. Experiments were performed with column volumes of 40.4, 80.6, and 121.2 mL (2, 4, and 6 CPC-LLN cartridges, respectively). The overall volumetric mass-transfer coefficient appears to be independent of the column volume, within the experimental error. A separation system can therefore be tested with a relatively small column volume (small retention times), and based on the model, a Péclet number, a partition coefficient, and an over-

Table 3. Overall Volumetric Mass-Transfer Coefficients for CMP and DCP for Various Column Volumes

Column Vol. mL	$k_o a$ (CMP) s^{-1}	$k_o a$ (DCP) s^{-1}
40.4	0.070 ± 0.007	0.024 ± 0.002
80.6	0.075 ± 0.007	0.029 ± 0.003
121.2	0.072 ± 0.007	0.029 ± 0.003

Note: $\epsilon_s = 0.57$; $\phi_v = 4$ mL/min; $\omega = 41$ rad/s; HMW 25 two-phase system.

all volumetric mass-transfer coefficient the optimum column volume (where separation is just sufficient) for a given separation can be estimated.

If the dimensions of the individual channels change, the column volume and the interfacial area (for an equal number of channels) will also change. Since the interfacial area depends on the type of flow regime that is present in a channel (Van Buel et al., 1995), it is (as yet) not possible to determine what will happen to $k_o a$ if the geometry of the channel is changed.

Relative contribution of dispersion, mass-transfer limitation, and off-column mixing on peak width

The results presented earlier clearly indicate that peak broadening is due to axial dispersion, mass-transfer limitation, and off-column mixing. To determine the relative contributions these phenomena have on the total peak width, simulations have been performed varying the following parameters: V, K, $k_s a$, and $k_m a$. The relative contributions to peak broadening have been determined by dividing the peak width (in seconds, at 0.607 of the peak height) caused by the three individual peak-broadening phenomena by the peak width of a simulated peak for which all three peak-broadening phenomena were taken into account. An experimental peak was used to determine the influence of off-column mixing. The influence of the flow rate, rotational acceleration, and the stationary-phase holdup is incorporated via their influence on $k_s a$ and $k_m a$. Figure 10 shows the relative contributions as a function of $k_s a$ and $k_m a$. For simplicity, the local volumetric mass-transfer coefficients are considered equal ($k_s a = k_m a$). The simulations were performed for a partition coefficient of 1, a Péclet number of 4,550, a flow rate of 4 mL/min, and a stationary-phase holdup of 0.55. A Péclet number of 4,550 is the average value found in Table 2. The volume was 121.2 mL, which is the smallest volume that is commonly used for separations in lab-scale equipment (6 CPC-LLN cartridges). The simulations were performed for $k_s a$ and $k_m a$ in the range 0.01–0.25 s, which is roughly the range for the heptane/methanol/water system for various phase compositions, rotational frequencies, and flow rates. Figure 10 clearly shows that mass-transfer limitation is the

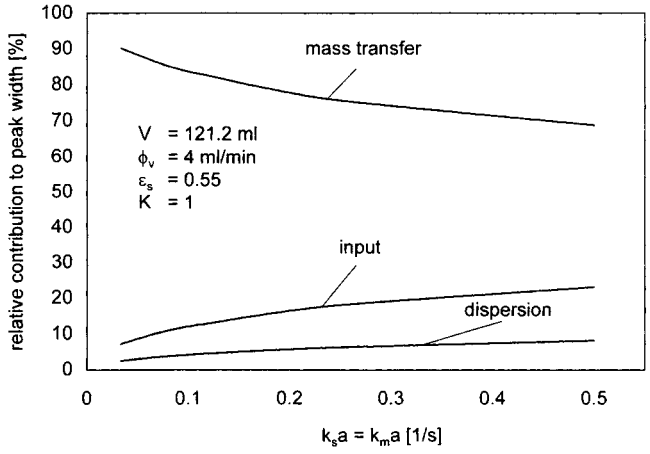

Figure 10. Relative contributions to peak broadening as a function of $k_s a$ and $k_m a$.

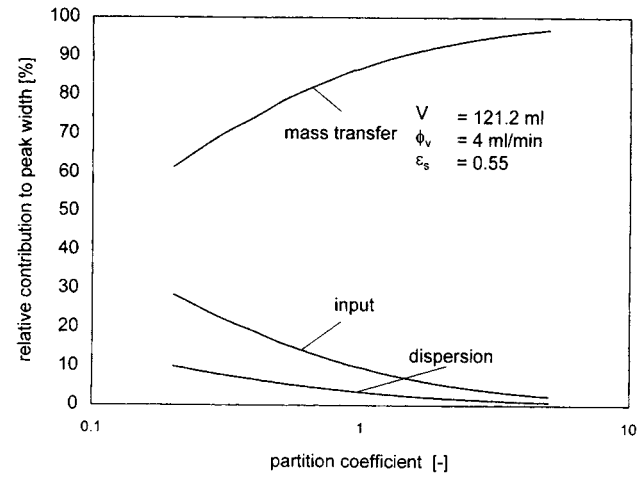

Figure 11. Relative contributions to peak broadening as a function of K.

main reason for peak broadening. Peak broadening due to off-column mixing and dispersion is constant as a function of $k_s a$ and $k_m a$, while the peak broadening due to mass-transfer limitation increases at higher values for $k_s a$ and $k_m a$.

Figure 11 shows the relative contributions as a function of the partition coefficient for the same experimental conditions as Figure 10. The overall volumetric mass-transfer coefficient (as a function of K) was calculated using the $1/k_s a$ and $1/k_m a$ values obtained from Figure 8. The simulations were performed for partition coefficients in the range of 0.2–5, which is considered the useful range for CPC separations. Peak broadening due to off-column mixing and dispersion are constant as a function of the partition coefficient. However, the mass-transfer limitation increases according to Eq. 10. Components with low partition coefficients elute almost unretained from the column, while components with higher partition coefficients elute from the column very broadly due to the high mass-transfer limitation. Therefore, the relative contribution due to mass-transfer limitation will increase if the partition coefficient increases.

Peak broadening due to off-column mixing is not a function of the column volume, while peak broadening due to mass transfer limitation and dispersion is a function of the column volume. This means that the relative contribution due to off-column mixing will decrease with increasing column volume. An increased channel volume (for a constant column volume) might lead to more mixing (lower Pe), which will increase the contribution due to dispersion of the mobile phase.

Since the contribution of off-column mixing and dispersion is minor, the analytical solution for the plug-flow model without dispersion and off-column mixing (Van Buel et al., 1996) will give fair results for most separation conditions.

Conclusions

The work presented in this article illustrates the possibility for modeling CPC effluent concentration profiles. Peak broadening is assumed to be caused by mass-transfer limitation, dispersion, and off-column mixing. The model describes the experimental concentration profiles accurately. Off-col-

umn mixing is characterized by performing pulse-response experiments without the column present in the experimental setup. Péclet numbers were determined, to characterize dispersion in the column. The Péclet numbers obtained from fitting the experiments are large (low dispersion). The Péclet number is (within the experimental error) independent of the flow rate, rotational frequency, stationary-phase holdup, and column volume.

Partition coefficients determined by fitting experimental concentration profiles with the model compare well ($r = 0.9983$) to partition coefficient determined by shake-flask experiments. The inverse overall volumetric mass-transfer coefficient is a linear function of the partition coefficient according to Eq. 10. From the slope and intercept with the y-axis, the volumetric mass-transfer coefficients in the mobile and stationary phase, respectively, are calculated. From the model predictions, it can be concluded that mass-transfer limitation is the main cause for peak broadening (> 65%).

By measuring the overall volumetric mass-transfer coefficient as a function of the various experimental conditions, the performance of a given two-phase system can be optimized with respect to the experimental conditions. Furthermore, it is possible to compare different two-phase systems and column geometries on the basis of their mass-transfer performance.

Acknowledgments

We thank the Department of Pharmacognosy of the Leiden University for providing the CPC-LLN cartridges. We also thank the technicians of the Kluyverlaboratory of the Delft University of Technology for constructing the rotor.

Literature Cited

Armstrong, D. W., G. L. Bertrand, and A. Berthod, "Study of the Origin and Mechanism of Band Broadening and Pressure Drop in Centrifugal Partition Chromatography," *Anal. Chem.*, **60**, 2513 (1988).

Berthod, A., and D. W. Armstrong, "Centrifugal Partition Chromatography: I. General Features," *J. Liq. Chromatog.*, **11**, 547 (1988a).

Berthod, A., and D. W. Armstrong, "Centrifugal Partition Chromatography: IV. Preparative Sample Purification and Partition Coefficient Determination," *J. Liq. Chromatog.*, **11**, 1187 (1988b).

Berthod, A., R. A. Menges, and D. W. Armstrong, "Direct Octanol Water Partition Coefficient Determination using Co-current Chromatography," *J. Liq. Chromatog.*, **15**, 2769 (1992).

Brigham, E. O., *The Fast Fourier Transform and Its Applications*, Prentice Hall, Englewood Cliffs, NJ (1988).

Conway, W. D., "Overview of Countercurrent Chromatography," *ACS Symp. Ser.*, **593**, 1 (1995).

El Tayar, N., R.-S. Tsai, P. Vallat, C. Altomare, and B. Testa, "Measurements of Partition Coefficients by Various Centrifugal Partition Chromatographic Techniques," *J. Chromatog. A*, **556**, 181 (1991).

Foucault, A. P., "Countercurrent Chromatography," *Anal. Chem.*, **64**, 569A (1991).

Foucault, A. P., "CPC Instrumentation," *Handbook of Centrifugal Partition Chromatography*, A. P. Foucault, ed., Dekker, New York, p. 355 (1995).

Gluck, S. J., and E. J. Martin, "Assessment of Centrifugal Partition Chromatography for Determination of Octanol-Water Partition Coefficients," *J. Liq. Chromatog.*, **13**, 2529 (1990).

Hsu, J. T., and T.-L. Chen, "Theoretical Analysis of the Asymmetry in Chromatographic Peaks," *J. Chromatog. A*, **404**, 1 (1987).

Lewis, W. K., and W. G. Whitman, "Principles of Gas Absorption," *Ind. Eng. Chem.*, **16**, 1215 (1924).

Marston, A., and K. Hostettmann, "Counter-Current Chromatography as a Preparative Tool," *J. Chromatog. A*, **658**, 315 (1994).

Sanki Laboratories, Inc., sales information.

van Buel, M. J., L. A. M. van der Wielen, and K. Ch. A. M. Luyben, "Pressure Drop in Centrifugal Partition Chromatography," *Handbook of Centrifugal Partition Chromatography*, A. P. Foucault, ed., Dekker, New York, p. 51 (1995).

van Buel, M. J., L. A. M. van der Wielen, and K. Ch. A. M. Luyben, "Modelling of Centrifugal Partition Chromatography," *Proc. Solvent Extraction Conf.*, D. C. Shallcross, R. Paimin, and L. M. Prvcic, eds., 1263 (1996).

Appendix: Solution of the CPC Model in the Fourier Domain

Simplifying Eqs. 15 and 16 leads to:

$$\frac{\partial X}{\partial \Theta} - \beta \frac{\partial^2 X}{\partial z} + \frac{\partial X}{\partial z} = -\gamma (X - Y) \tag{A1}$$

$$\frac{\partial Y}{\partial \Theta} = \frac{1}{\alpha}(X - Y), \tag{A2}$$

where

$$\alpha = \frac{1}{St} \frac{\epsilon_s}{(1 - \epsilon_s)} \tag{A3}$$

$$\beta = \frac{1}{Pe} \tag{A4}$$

$$\gamma = St\, K. \tag{A5}$$

Transforming Eq. A2 to the Laplace domain gives

$$s\tilde{Y} - \tilde{Y}_{+o} = \frac{1}{\alpha}(\tilde{X} - \tilde{Y}). \tag{A6}$$

From boundary Eq. 3 it follows that

$$\tilde{Y}_{+o} = 0. \tag{A7}$$

This leads to

$$\tilde{Y} = \frac{1}{(\alpha s + 1)} \tilde{X}. \tag{A8}$$

Transforming Eq. A1 to the Fourier domain and using boundary Eq. 4 leads to

$$-\beta \frac{d^2 \tilde{X}}{dz^2} + \frac{d\tilde{X}}{dz} + s\tilde{X} = -\gamma (\tilde{X} - \tilde{Y}). \tag{A9}$$

Substituting Eq. A8 in Eq. A9 leads to

$$-\beta \frac{d^2 \tilde{X}}{dz^2} + \frac{d\tilde{X}}{dz} + \left(\frac{\alpha s^2 + \alpha \gamma s + s}{\alpha s + 1} \right) \tilde{X} = 0. \tag{A10}$$

The solution of differential Eq. A10 is

$$\tilde{X} = C_1 \exp\frac{1}{2}\frac{\left(\alpha s+1-\sqrt{\alpha^2 s^2+2\alpha s+1+4\beta\alpha^2 s^3+4\beta\alpha^2 s^2\gamma+8\alpha\beta s^2+4\alpha\beta\gamma s+4\beta s}\right)z}{\beta(\alpha s+1)} + C_2 \exp\frac{1}{2}\frac{\left(\alpha s+1+\sqrt{\alpha^2 s^2+2\alpha s+1+4\beta\alpha^2 s^3+4\beta\alpha^2 s^2\gamma+8\alpha\beta s^2+4\alpha\beta\gamma s+4\beta s}\right)z}{\beta(\alpha s+1)} \tag{A11}$$

Applying boundary Eqs. 5 and 6 gives

$$C_1 = 1$$
$$C_2 = 0.$$

A solution for X in the Fourier domain can be obtained by substituting $j\omega$ for s, which leads to

$$\tilde{X} = \exp\frac{1}{2}\frac{\left(\alpha j\omega+1-\sqrt{-\alpha^2\omega^2+2\alpha j\omega+1-4\alpha^2\beta j\omega^3-4\alpha^2\beta\gamma\omega^2-8\alpha\beta\omega^2+4\alpha\beta\gamma j\omega+4\beta j\omega}\right)z}{\beta(j\alpha\omega+1)} \tag{A12}$$

The real and imaginary parts of Eq. A12 are

$$Re(X) = \exp\left(\frac{1}{2}\frac{zA_1}{\beta(1+\alpha^2\omega^2)}+\frac{1}{2}\frac{zA_2\alpha\omega}{\beta(1+\alpha^2\omega^2)}\right)\cos\left(\frac{1}{2}\frac{zA_2}{\beta(1+\alpha^2\omega^2)}-\frac{1}{2}\frac{zA_1\alpha\omega}{\beta(1+\alpha^2\omega^2)}\right) \tag{A13}$$

$$Im(X) = \exp\left(\frac{1}{2}\frac{zA_1}{\beta(1+\alpha^2\omega^2)}+\frac{1}{2}\frac{zA_2\alpha\omega}{\beta(1+\alpha^2\omega^2)}\right)\sin\left(\frac{1}{2}\frac{zA_2}{\beta(1+\alpha^2\omega^2)}-\frac{1}{2}\frac{zA_1\alpha\omega}{\beta(1+\alpha^2\omega^2)}\right), \tag{A14}$$

where

$$A_1 = 1-\frac{1}{2}\sqrt{2A_3-2\alpha^2\omega^2+2-8\alpha^2\beta\gamma\omega^2-16\alpha\beta\omega^2} \tag{A15}$$

$$A_2 = \alpha\omega-\frac{1}{2}A_4\sqrt{2A_3+2\alpha^2\omega^2-2+8\alpha^2\beta\gamma\omega^2+16\alpha\beta\omega^2} \tag{A16}$$

$$A_3 = \sqrt{(-\alpha^2\omega^2+1-4\alpha^2\beta\gamma\omega^2-8\alpha\beta\omega^2)^2+(2\alpha\omega-4\alpha^2\beta\omega^3+4\alpha\beta\gamma\omega+4\beta\omega)^2} \tag{A17}$$

$$\begin{aligned} A_4 &= 1 \quad \text{if} \quad A_5>0 \quad \text{or if } A_5=0 \text{ and } A_6>0 \\ A_4 &= -1 \quad \text{if} \quad A_5<0 \quad \text{or if } A_5=0 \text{ and } A_6<0 \\ A_4 &= 0 \quad \text{if} \quad A_5=0 \quad \text{and } A_6=0 \end{aligned} \tag{A18}$$

$$A_5 = 2\alpha\omega-4\alpha^2\beta\omega^3+4\alpha\beta\gamma\omega+4\beta\omega \tag{A19}$$

$$A_6 = \alpha^2\omega^2-1+4\alpha^2\beta\gamma\omega^2+8\alpha\beta\omega^2. \tag{A20}$$

Manuscript received June 19, 1996, and revision received Sept. 5, 1996.